THE PHOTOLYSIS OF 1-IODOPROPANE

ROBERT W. CARR, JR., and MICHAEL G. TOPOR

Department of Chemical Engineering and Materials Science, University of Minnesota, Minneapolis, MN 55455 (U.S.A.)

(Received October 7, 1980; in revised form December 17, 1980)

Summary

Photodissociation of 1-iodopropane vapor was studied at 265, 236.5, 222.4 and 214 nm. In all cases highly vibrationally excited *n*-propyl radicals were formed. Excited *n*-propyl radical dissociation to methyl radicals and ethylene was observed at all wavelengths shorter than 265 nm; evidence was obtained for a dissociation pathway of lesser signficance to hydrogen atoms and propylene.

Model calculations indicated that the photodissociation occurs by an impulsive mechanism and that a population inversion of $I(^2P_{1/2})$ and $I(^2P_{3/2})$ occurs at all wavelengths. Furthermore, the calculations suggest that the inversion is smaller at 214 nm than at wavelengths which are in the 1-iodopropane A band.

1. Introduction

The photolysis of simple alkyl iodides yields alkyl radicals with large non-equilibrium amounts of energy. Energized methyl radicals from methyl iodide exhibit enhanced reactivity toward hydrogen atom abstraction [1], and quantum yields for hydrogen atom abstraction from several substances by hot ethyl radicals, formed during ethyl iodide photolysis at 253.7 and 228.8 nm, have been reported [2]. Decomposition of excited *n*-propyl radicals results from *n*-propyl iodide photolysis with the unfiltered emission of a medium pressure mercury arc [3] and from photolysis at 147 nm [4]. In ref. 3 the excited *n*-propyl radicals were suggested to be capable of hydrogen atom abstraction to account for propane formation. Photofragment spectroscopy has been applied [5] to methyl, ethyl, *n*-propyl and isopropyl iodides. The translational energy distribution in the center of mass of the recoiling fragments was measured following 266.2 nm excitation, from which the internal energy distribution of the corresponding alkyl radical was deduced by application of total energy conservation.

0047-2670/81/0000-0000/$02.50

Another feature of the primary process in alkyl iodides is the production of both $I(5^2P_{1/2})$ atoms and $I(5^2P_{3/2})$ atoms. Lasing action on the $I(5^2P_{1/2}) \rightarrow I(5^2P_{3/2})$ transition has been observed [6] in *n*-propyl iodide, and $I(5^2P_{1/2})$ has been detected [7] following flash photolysis of *n*-propyl iodide. More recently the relative yields of $I(5^2P_{1/2})$ and $I(5^2P_{3/2})$ have been measured [8] in flash photolysis.

In this paper an investigation of 1-iodopropane photolysis is reported. If the *n*-propyl radicals expected from the primary process contain internal energy in excess of the threshold energy for dissociation, measurement of the radical dissociation products as a function of pressure is expected to yield information on energy partitioned into internal degrees of freedom of the propyl radical. Thus this technique complements photofragment spectroscopy. By working near 266 nm the present results could be compared with those from photofragment spectroscopy [5]. Four wavelengths in the A band [9] ($\lambda_{max} \approx 250$ nm) were selected for study. A systematic study of product quantum yields from *n*-propyl iodide has not yet been reported in this region to our knowledge. In addition, one wavelength at the onset of the second absorption region (B and C bands at about 200 nm) [9] was chosen to see whether there were significant differences in the photochemistry of these two regions.

2. Experimental

2.1. Apparatus

A mercury-free vacuum system pumped by a two-stage oil diffusion pump maintained a pressure of 10^{-5} Torr. A Wallace and Tiernan 0 - 220 Torr differential pressure gauge measured reactant pressures. Two cylindrical Pyrex reactors, one with planar Suprasil end windows and the other with Ultrasil windows, were used. The former was 16.4 cm long with an inner diameter of 3.10 cm (120.8 cm^3) and the latter was 18.3 cm long with an inner diameter of 3.10 cm (138.3 cm^3). The 222.4, 236.5, 265.0, 302.5 and 313.0 nm regions were isolated from the emission of a 550 W medium pressure mercury arc with a Bausch and Lomb high intensity grating monochromator, using slit widths giving a 100 Å bandpass. The 214.0 nm emission of a 16 W zinc arc was isolated using a 4 cm path of chlorine at 1 atm. An RCA 935 photodiode was used to monitor light intensity.

2.2. Actinometry

Radiant fluxes at 214.0, 222.4 and 236.5 nm were measured by HBr actinometry [10]. The flux at 265.0 nm was measured using ketene photolysis at 300 K as an actinometer and accepting $\Phi(CO) = 2$ [11]. The H_2 yields from the HBr actinometer and the CO yields from the ketene actinometer were measured with a Toepler pump.

2.3. Product analysis

A Barber–Colman series 5000 gas chromatograph with a flame ionization detector was used for all analyses. Routine analyses were carried out on a column 10 ft in length and $\frac{1}{4}$ in in outer diameter which was packed with 80/100 mesh Propak Q and was operated at 408 K with 130 cm^3 min^{-1} of helium carrier at 54 lbf in^{-2}. Retention times and calibration factors were determined from mixtures of authentic samples. Additionally, qualitative analysis of alkyl iodides was performed on a column 2 ft in length and $\frac{1}{4}$ in in outer diameter containing 15 wt.% tricresylphosphate on 60/80 mesh Chromosorb W at 298 K, 20 lbf in^{-2} and 30 cm^3 min^{-1} of helium. Product yields were determined by an internal standard method using small (usually below 0.4%) accurately measured amounts of *n*-butane or *n*-pentane as the standard.

2.4. Chemicals

Eastman White Label 1-iodopropane was repeatedly washed with aliquots of 0.1 N $Na_2S_2O_3$ followed by drying with $CaSO_4$. Washings were continued until the 478.0 nm I_2 absorption band was no longer detectable in a 10 cm path by spectrophotometry. The washed product was pumped under vacuum at 250 K. Analysis by gas chromatography on Propak Q showed less than 0.1% of an unidentified C_6 hydrocarbon and analysis on tricresylphosphate indicated the presence of less than 0.1% of iodopropane and no detectable decomposition products.

Matheson HBr with a stated purity of 99.8% was used. Ketene was prepared by pyrolysis of acetic anhydride [12]. *n*-Butane and *n*-pentane were Phillips research grade materials which were shown by gas chromatographic analysis to be free of detectable impurities. Both were degassed by vacuum pumping while being maintained at −78 °C. Nitrogen (Airco high purity grade) and oxygen (National Cylinder gas tank grade) were both employed without further purification.

3. Results

3.1. Products

The products observed were ethylene, propylene, propane and methyl iodide. Traces of methane were detected at low pressures in short-wavelength experiments. No C_6 hydrocarbons were found under any conditions. Attempts to detect molecular iodine and hydrogen iodide by both spectrophotometry and gas chromatography were frustrated by insufficient instrument sensitivity.

3.2. Added gases

The effect of added oxygen was investigated at 222.4 nm by photolyzing mixtures of 1-iodopropane and oxygen in varying proportions at approximately constant total pressure. The results in Table 1 show that the

TABLE 1

The effect of added gases at 222.4 nm

Total pressure (Torr)	*Added gas* (mole fraction)		*Quantum yield*			
	O_2	N_2	*Ethylene*	*Propylene*	*Propane*	*Methyl iodide*
20.8	0.0	0.0	0.095	0.041	0.043	0.063
21.0	0.26	0.0	0.10	0.097	Trace	0.013
21.0	0.50	0.0	0.10	0.112	Trace	0.024
27.5	0.015	0.0	0.085	0.066	0.002	0.023
27.6	0.015	0.19	0.11	0.086	Trace	0.054
28.0	0.015	0.51	0.10	0.082	Trace	0.065
28.4	0.015	0.66	0.12	0.079	Trace	(0.16)[a]
28.0	0.015	0.74	0.12	0.077	0.004	(0.12)[a]
28.1	0.015	0.88	0.12	0.089	Trace	—

[a]Quantum yield untrustworthy.

quantum yield of ethylene is independent of oxygen concentration and that propane formation is virtually completely suppressed by oxygen. Methyl iodide quantum yields decreased but were not completely eliminated.

Mixtures of 1-iodopropane and nitrogen at approximately constant total pressure and containing 1.5 mol.% O_2 were photolyzed at 222.4 nm. Quantum yields of propane were suppressed as in the oxygen-containing experiments and quantum yields of ethylene, propylene and methyl iodide were independent of the nitrogen mole fraction.

3.3. Pressure

Since added nitrogen up to 88 mol.% had no observable effect on the product quantum yields, nitrogen was used to extend the pressure range of the experiments beyond the vapor pressure of 1-iodopropane.

The effect of pressure on ethylene quantum yields at 214.0, 222.4 and 236.5 nm is shown in Fig. 1 and that at 265.0 nm is shown in Fig. 2. At all four wavelengths the quantum yields increase with decreasing pressure. Furthermore, ethylene quantum yields at any given pressure increase with increasing photon energy.

Propylene quantum yields are shown in Fig. 3. At 214 and 222.4 nm the quantum yields increase with decreasing pressure and at any given pressure they are larger at higher photon energies. At 236.5 nm there may be a slight increase at pressures below 1 Torr but the scatter is such that no definite claim for a pressure dependence can be made. The data at 265.0 nm appear to be independent of pressure from 400 to 0.2 Torr.

The 214.0 and 222.4 nm propylene quantum yields plotted against reciprocal pressure showed small positive intercepts of about 0.05. Thus it appears that there is also a pressure-independent source of propylene at these wavelengths which is comparable in size with the pressure-independent source at 236.5 and 265 nm. Plots of the ethylene quantum yield *versus*

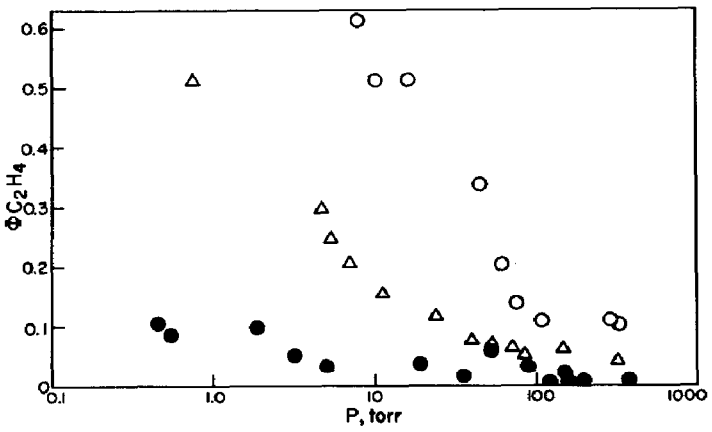

Fig. 1. Pressure dependence of ethylene quantum yields: ○, 214 nm; △, 222.4 nm; ●, 236.5 nm.

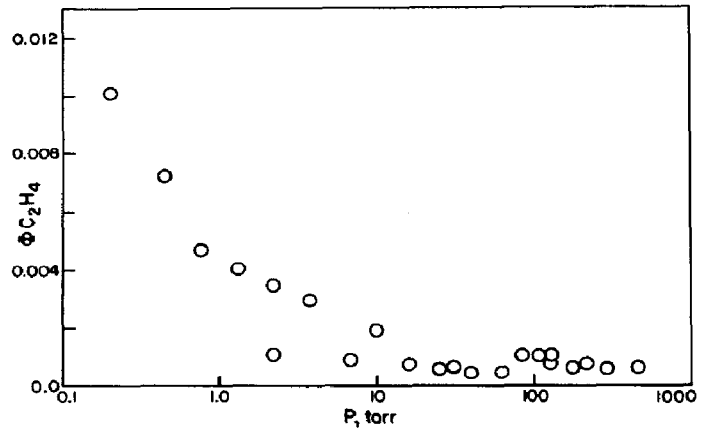

Fig. 2. Pressure dependence of ethylene quantum yields at 265 nm.

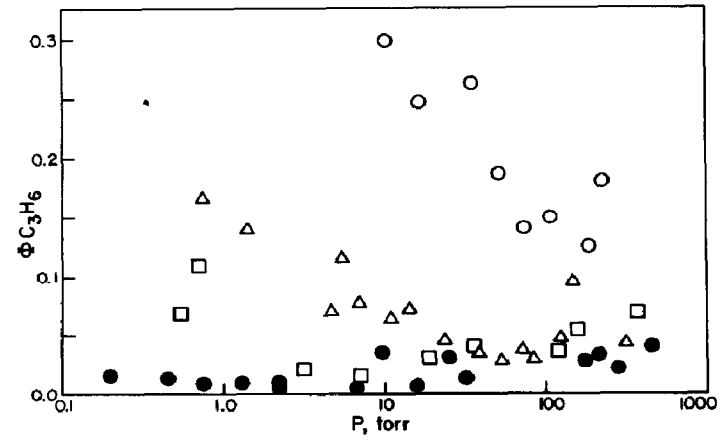

Fig. 3. Pressure dependence of propylene quantum yields: ○, 214 nm; △, 222.4 nm; □, 236.5 nm; ●, 265 nm.

reciprocal pressure showed considerable curvature near the origin. They appeared to have zero intercepts although small non-zero intercepts could not be ruled out.

Methyl iodide quantum yields also increased with decreasing pressure at 265.0 nm and higher photon energies. Ethylene and methyl iodide have the same pressure and wavelength dependences.

Propane quantum yields were extremely sensitive to trace amounts of oxygen. The data showed considerable scatter, presumably for this reason, and are not reported here. No clear-cut trends with pressure could be detected, although the quantum yields increased with decreasing wavelength from below 0.01 at 265 nm to about 0.35 at 214 nm.

4. Discussion

4.1. Mechanism

Excitation of transitions in the A band results in dissociation of the C—I bond [1]. The predicted [13] formation of electronically excited iodine atoms has recently been detected [6] by observation of the 206.2 nm absorption line of $I(5^2P_{1/2})$ and $I(5^2P_{3/2})$ states. The excess photon energy in the 250 nm band results in both translational and internal excitation of the *n*-propyl radical [3, 5]:

$$n\text{-}C_3H_7I + h\nu \rightarrow n\text{-}C_3H_7^* + I(5^2P_{1/2}) \quad (1)$$

$$n\text{-}C_3H_7I + h\nu \rightarrow n\text{-}C_3H_7^* + I(5^2P_{3/2}) \quad (2)$$

The fate of the excited radical is either dissociation via methyl or hydrogen atom elimination (reactions (3) and (4)), provided that the internal energy of $n\text{-}C_3H_7^*$ is greater than about 31 kcal mol^{-1} and 37 kcal mol^{-1} respectively [14], or collisional deactivation.

$$n\text{-}C_3H_7^* \rightarrow CH_3 + C_2H_4 \quad (3)$$

$$n\text{-}C_3H_7^* \rightarrow H + C_3H_6 \quad (4)$$

The observation here that ethylene and propylene quantum yields are unaffected by added oxygen must mean that they are not formed by a mechanism involving thermally equilibrated free radicals. The pressure dependence of ethylene and propylene quantum yields is consistent with the intermediacy of photochemically activated propyl radicals. Furthermore, $[C_2H_4]/[C_3H_6] > 1$ at 214 and 222.4 nm, in qualitative agreement with the lower threshold energy of ethylene formation.

In Table 2 some thermochemistry and energetics of the 1-iodopropane system are summarized. The excess photon energies E_{exc} and E'_{exc} are calculated from

$$E_{exc} = h\nu + E_{int} - D_0^\circ \quad (5)$$

TABLE 2

Thermochemistry and energetics

	Energy (kcal mol^{-1})			
	265.0 nm	*236.5 nm*	*222.4 nm*	*214.0 nm*
$h\nu$	108.0	121.0	129.0	134.0
E_{exc}	57.4	70.4	78.4	83.4
E'_{exc}	35.7	48.7	56.7	61.7
$\langle E \rangle$[a]	30.4	37.3	41.6	44.2
$\langle E' \rangle$[a]	19.0	25.8	30.1	32.7

[a] 53% of the excess photon energy is assumed to be partitioned into internal degrees of freedom of the propyl radical.

$$E'_{exc} = h\nu + E_{int} - D_0^\circ - 21.7 \quad (6)$$

and correspond to the maximum energies available for vibrational excitation of propyl radicals accompanying the formation of respectively ground and excited state iodine atoms. In eqns. (5) and (6) $h\nu$ is the energy of an einstein of photons, E_{int} is the thermal equilibrium internal energy of propyl radicals at 300 K (2.0 kcal mol^{-1}), D_0° is the n-C_3H_7—I bond dissociation energy (52.6 kcal mol^{-1}) and 21.7 kcal mol^{-1} is the iodine atom excitation energy. Riley and Wilson [5] have reported that about 53% of the excess photon energy is partitioned into internal degrees of freedom of the propyl radical during n-C_3H_7I photolysis at 266 nm. If the same 53% partitioning is applied at each of the wavelengths employed here, the average energies $\langle E \rangle$ and $\langle E' \rangle$ of the propyl radicals formed with $I(^2P_{3/2})$ and $I(^2P_{1/2})$ respectively can be calculated. These are also included in Table 2. The excess photon energy from reaction (2) is sufficient to allow both ethylene and propylene formation by reactions (3) and (4) at all six wavelengths. From reaction (1), however, there is insufficient excess photon energy for propylene formation via reaction (4) at 265.0 nm. The pressure dependence of ethylene quantum yields at 214, 222.4, 236.5 and 265 nm is consistent with the energetics of the formation of both $I(^2P_{1/2})$ and $I(^2P_{3/2})$ followed by reaction (3). Propylene quantum yields show a clear pressure dependence only at 214 and 222.4 nm, also consistent with the energetics of $I(^2P_{1/2})$ and $I(^2P_{3/2})$ formation followed by reaction (4). Furthermore, the lack of dependence of ethylene and propylene yields on added oxygen is consistent with their formation from reactions (3) and (4). Finally, the fact that propylene quantum yields are pressure independent at longer wavelengths must mean that, if $I(^2P_{3/2})$ atoms are also formed in the primary process, the propyl radicals accompanying them have insufficient energy to decompose.

A pressure-independent source of propylene is required at 265 and 236.5 nm and is strongly suggested at 214 and 222.4 nm from the non-zero intercepts of plots of $\Phi(C_3H_6)$ *versus* P^{-1}. Thrush [15] has observed strong absorption bands due to hydrogen iodide during flash photolysis of 1-iodo-

propane and has suggested that it might be formed from the molecular photodecomposition

$$n\text{-}C_3H_7I + h\nu \rightarrow C_3H_6 + HI \quad (7)$$

Schindler and Wijnen [16] have shown that hydrogen iodide elimination from ethyl iodide by full radiation from a mercury arc occurs with a quantum yield of 0.05, which is remarkably close to the pressure-independent propylene quantum yields found here, and Rebbert *et al.* [4] have suggested that reaction (5) occurs in the 147 nm photolysis of *n*-propyl iodide. However, McCauley and Hilsdorf [17] have found propylene formation by

$$I + n\text{-}C_3H_7 \rightarrow C_3H_6 + HI \quad (8)$$

in liquid phase photolysis at 253.7 nm; Guercione and Wijnen [18] have shown that in vapor phase photolysis of mixtures of methyl iodide and diethyl ketone, the pair of reactions

$$I + C_2H_5 \rightarrow C_2H_4 + HI \quad (9)$$

and

$$I + C_2H_5 \rightarrow C_2H_5I \quad (10)$$

occur with the rate constant ratio $k_9/k_{10} = 0.33 \pm 0.03$. In this work it is not possible to distinguish between reactions (7) and (8) and both may occur.

Abstraction of hydrogen atoms by hot *n*-propyl radicals, *i.e.*

$$n\text{-}C_3H_7^* + C_3H_7I \rightarrow C_3H_8 + C_3H_6I \quad (11)$$

has been suggested [3] to account for propane yields in the photolysis of 1-iodopropane by a full mercury arc. However, the present observation that only 1.5 mol.% added oxygen completely suppresses propane formation provides evidence that propane is formed by reactions of thermalized radicals. Furthermore, the propane yields are not noticeably affected by the presence of 80 mol.% added nitrogen.

The fate of $I(^2P_{1/2})$ atoms is spin–orbit deactivation to the ground state by collisions with (predominantly) 1-iodopropane [19]:

$$I(^2P_{1/2}) + n\text{-}C_3H_7I \rightarrow I(^2P_{3/2}) + n\text{-}C_3H_7I \quad (12)$$

Reactions (13) - (18) are the expected steps for the thermalized ground state atoms and radicals present:

$$CH_3 + n\text{-}C_3H_7I \rightarrow CH_3I + C_3H_7 \quad (13)$$

$$H + C_3H_7I \rightarrow HI + C_3H_7 \quad (14)$$

$$C_3H_7 + I(^2P_{3/2}) \rightarrow n\text{-}C_3H_7I \quad (15)$$

$$2I(^2P_{3/2}) + M \rightarrow I_2 + M \quad (16)$$

$$C_3H_7 + I_2 \rightarrow C_3H_7I + I(^2P_{3/2}) \quad (17)$$

$$C_3H_7 + HI \rightarrow C_3H_8 + I(^2P_{3/2}) \quad (18)$$

If reaction (13) is the only route for removal of methyl radicals, the ratio of methyl iodide to ethylene is predicted to be unity. This is approximately so at 265.0 and 236.5 nm; however, the ratio is less than unity at 222.4 and 214.0 nm, indicating that methyl radicals may react by an additional path at short wavelengths.

4.2. Stochastic model

Some information on energy partitioned into the propyl radical was obtained by RRKM calculations of the dissociation to ethylene. The quantum yield for ethylene formation is given by

$$\Phi(C_2H_4) = \sum_{\phi_i} [k\{k + \omega(I - P)\}^{-1}F]_i \qquad (19)$$

This results from a stationary stochastic model of the net rate of formation of energized propyl radicals having discrete energy levels i. $\Phi(C_2H_4)$ is related to experiment by $\Phi(C_2H_4) = D/(D + S)$, where ϕ is the primary photodissociation quantum yield and D and S are the decomposition and stabilization yields respectively. In eqn. (19) k is a main diagonal matrix with the unimolecular rate constants k_i as elements, F is the normalized activation distribution of excited species, I is the unit matrix and P is the matrix of collisional transition probabilities P_{ij}. The values of k_i were computed from RRKM theory [20], the step-ladder model, where the principles of detailed balance and completeness were followed, was used for the values of P_{ij} and two models, an impulsive model and a statistical model, were used to deduce the distribution function. The molecular models used for calculation of microscopic rate constants are given in Appendix A. These molecular models were used to calculate the decomposition-to-stabilization ratio for *n*-propyl radicals chemically activated by addition of hydrogen atoms to the secondary carbon of propylene. Using a step-ladder model for deactivation, with a step size of 9.1 kcal mol^{-1}, satisfactory agreement with the data given in ref. 21 was obtained.

4.3. Internal energy distribution

The internal energy distribution of the dissociating *n*-propyl radicals was modeled for two limiting cases which may be calculated *a priori:* a statistical model and an impulsive model. These distributions constitute two types of trial function to be used in the calculations. In addition, calculations using a distribution derived from the 266 nm translation energy distributions of Riley and Wilson [5], obtained by photofragment spectroscopy, were carried out for comparison with our 265 nm data.

The strategy used in these calculations was not to fit the data to deduce a detailed energy distribution function but rather to use model calculations to bound the data to see what general conclusions might be reached on energy partitioning. We consider that the number of parameters to be used in fitting, $\langle E \rangle$, $\langle \Delta E \rangle$ and $[I(^2P_{1/2})]/[I(^2P_{3/2})]$, precludes obtaining unique energy distribution functions.

If the excess photochemical energy were partitioned statistically among the available degrees of freedom of each fragment, the energy distribution of the propyl radical would be relatively wide. If we let $f(E)$ represent the propyl radical activation distribution and N_p and N_I represent the state densities for the degrees of freedom for the radical and atom respectively, then for the total amount of available excess energy E_{exc} [22]

$$f(E) = \frac{N_p(E)N_I(E_{exc} - E)}{\sum_{i=0}^{E_{exc}} N_p(i)N_I(E_{exc} - i)}$$

where E_{exc} is given by the sum of the photon energy $E_{h\nu}$ and the 1-iodopropane thermal energy (assumed to be 2.1 kcal mol^{-1} at 25 °C) minus the C—I bond dissociation energy at 0 K (52.6 kcal mol^{-1}).

$$E_{exc} = E_{h\nu} - 50.5 \text{ kcal mol}^{-1}$$

If the electronic degrees of freedom are excluded from N_I, then the distribution can be calculated with E_{exc} for radicals which yield ground state iodine atoms and with E'_{exc} for radicals which yield excited state iodine atoms, where E'_{exc} is E_{exc} minus the electronic excitation energy of 21.7 kcal mol^{-1}:

$$E'_{exc} = E_{h\nu} - 72.2 \text{ kcal mol}^{-1}$$

An impulsive model can be deduced by considering that the excited state of 1-iodopropane is repulsive and, if the C—I bond leaves in one vibrational period, the excess energy appears entirely in C—I repulsion. There are two limiting cases: (1) the carbon atom bonded to iodine is very loosely attached to the rest of the radical; (2) the entire radical is totally rigid. In the first case the fraction of the available excess energy that this excitation represents is [5]

$$1 - \mu_a/\mu_b \approx 0.666$$

where μ_a is the reduced mass of the carbon and iodine atoms at either end of the breaking bond and μ_b is the reduced mass of the propyl radical and iodine atom.

In the second case the amount of excitation is approximately 0.340 of the available excess energy [5]. In the impulsive model calculation to follow, the average internal energy of the propyl radical is assumed to be an adjustable parameter which lies in the range $0.34E_{exc} \leqslant \langle E \rangle \leqslant 0.666E_{exc}$.

4.4. Photolysis at 265 nm

Figure 4 shows a Stern–Volmer plot of the 265 nm data. A somewhat uncertain extrapolation to zero pressure (due to severe curvature near the origin) indicates that $\{\Phi(C_2H_4)\}_{p=0}$ is at most about 0.1. Experiments at pressures lower than 0.2 Torr, where $\Phi(C_2H_4) = 0.01$, were not possible be-

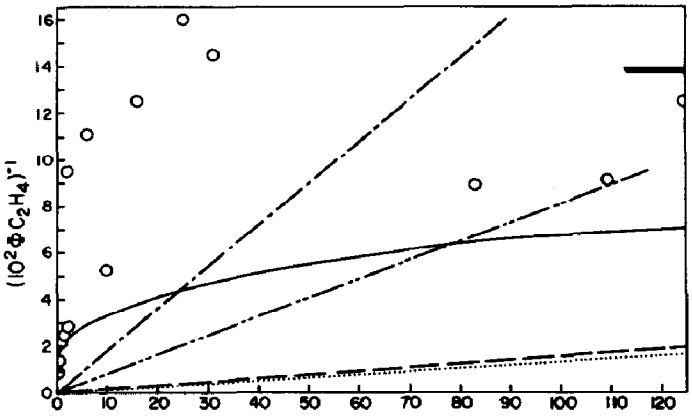

Fig. 4. Stern–Volmer plot of the 265 nm data (○); - - -, calculated using a statistical model, $\langle \Delta E \rangle$ = 2 kcal mol^{-1}; . . ., statistical model with strong collisions; – – –, calculated using an impulsive model, $\langle \Delta E \rangle$ = 1 kcal mol^{-1}; – – – –, impulsive model with strong collisions; ——, internal energy distribution derived from photofragment spectroscopy measurements, $\langle \Delta E \rangle$ = 9.1 kcal mol^{-1}; ——, average of five experiments between 120 and 450 mmHg. The pressure (mmHg) is given along the abscissa.

cause of lack of analytical sensitivity. Thus, at most, about 10% of the propyl radicals have energies above threshold.

Riley and Wilson [5] have found that *n*-propyl radicals formed at 266 nm contain on average 53% of the available excess photon energy as internal excitation when the other photofragment is assumed to be $I(^2P_{1/2})$. Table 2 shows that if the same partitioning occurs at 265 nm the average energy of the propyl radicals associated with $I(^2P_{1/2})$ formation would be significantly less than the threshold energy for decomposition to ethylene and that the radicals associated with $I(^2P_{3/2})$ formation would have an average energy of 30.4 kcal mol^{-1}, only slightly less than the threshold energy. The relatively narrow internal energy distribution predicted using the impulsive model (approximately 2 kcal mol^{-1}) then requires that ethylene formation at 265 nm must come only from those propyl radicals associated with $I(^2P_{3/2})$ formation. In the 265 nm calculations it is assumed that the propyl radicals which decompose are those associated with $I(^2P_{3/2})$ production.

Calculations with the statistical model for E_{exc} = 57.4 kcal mol^{-1} using both strong collisions and $\langle \Delta E \rangle$ = 2 kcal mol^{-1} are shown in Fig. 4. All the calculations at 265 nm used η = 0.01, where η is the fraction of iodine atoms in the ground state. This was necessary to account for the small ethylene quantum yields at this wavelength. The statistical model calculations are in serious disagreement with the data, so this model can be safely rejected. Impulsive model calculations gave linear Stern–Volmer plots for all deactivation step sizes, in contrast with the curvature of the data. The linearity is no doubt a result of the narrowness of the distribution given by the impulsive model. Also shown in Fig. 4 is an impulsive model calculation for 61% partition using two extremes of deactivation step size. Finally, a calculation using an internal energy distribution derived from the translational energy distribu-

tion of Riley and Wilson [5] and a step size of 9.1 kcal mol^{-1} [21] is shown. This distribution puts the required curvature into the calculated plot, as shown by the full curve in Fig. 4. There is reasonably good agreement with experiment at low pressures but the calculation overestimates $\Phi(C_2H_4)$ by about a factor of 2 at high pressures. Agreement with experiment could be forced at high pressures by cutting off the higher tail of the distribution, but this was not done. We conclude that the 265 nm results are in reasonably good agreement with the data of Riley and Wilson [5], provided that η = 0.01 is accepted. This is not unreasonable since the translational energy distribution showed only one peak, implying a small value of η. In the calculation the implicit assumption is made that the fraction of available energy which appears in the *n*-propyl radical as internal excitation is independent of whether $I(^2P_{1/2})$ or $I(^2P_{3/2})$ is produced. This is also not unreasonable and in fact was first suggested by Riley and Wilson [5].

Donahue and Wiesenfeld [8] have found η = 0.5 in broad-band flash photolysis of *n*-propyl iodide. Although the value of η = 0.01 at 265 nm suggested by the present experiments cannot be regarded as firmly established, it is tempting to suggest that η may increase with decreasing wavelength.

4.5. Photolysis at wavelengths shorter than 265 nm

Stern–Volmer plots of ethylene quantum yields at 236.5, 222.4 and 214.0 nm were compared with model calculations. For a particular deactivation step size a family of solutions of eqn. (19) was generated for each trial function representing the propyl radical internal energy distribution by varying a trial function parameter. For the statistical model the parameter was E'_{exc} and for the impulsive model it was $\langle E \rangle$. The members of each family best bounding the data were then selected.

Calculations for the statistical model were performed for $\langle \Delta E \rangle$ = 2 kcal mol^{-1} and for strong collisions. For either step size the data could only be fitted using values of E'_{exc} which are considerably less than the actual amounts of excess energy to be partitioned. Thus the statistical model can be ruled out on energetic grounds at short wavelengths also.

With the impulsive model, calculations assuming that all the iodine atoms are formed in one electronic state (either all ground state or all excited state) yield linear Stern–Volmer plots. To obtain curvature it was necessary to use bimodal distributions corresponding to formation of both $I(^2P_{3/2})$ and $I(^2P_{1/2})$. This, however, introduces an additional parameter, the iodine atom branching ratio $[I(^2P_{1/2})]/[I(^2P_{3/2})]$.

Impulsive model calculations were carried out by letting the average internal energy of the propyl radicals associated with $I(^2P_{3/2})$ formation be a constant 12 kcal mol^{-1} higher than those associated with $I(^2P_{1/2})$ formation. Thus slightly more than half the 21.7 kcal mol^{-1} electronic excitation of iodine atoms goes to the propyl radical internal excitation when a ground state iodine atom is produced, as is the case at 265 nm [5]. Thus an activation distribution trial function is obtained which has two narrow peaks (ap-

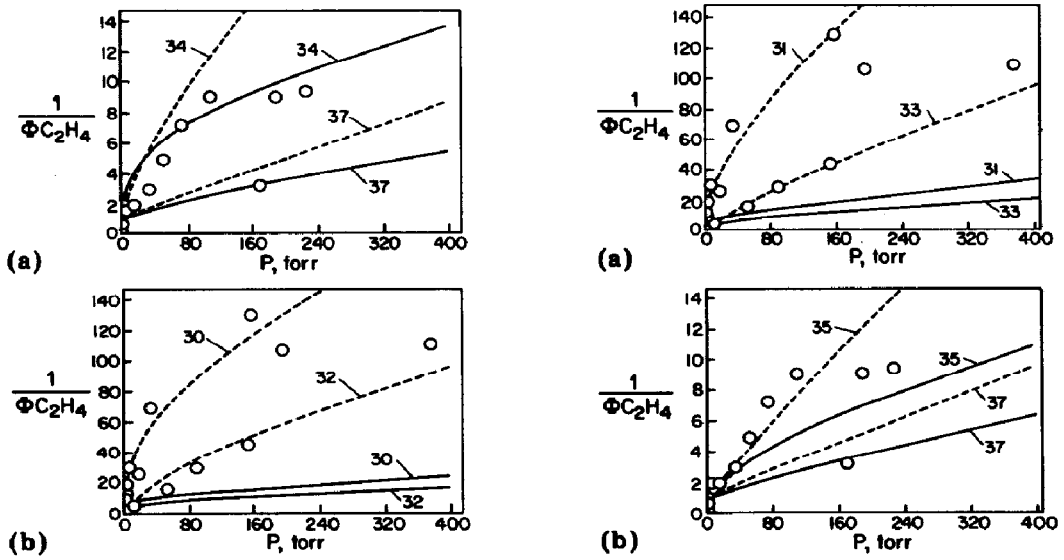

Fig. 5. Stern–Volmer plots. (a) ○, 214 nm data;——, $\eta = 0.1$, $\langle \Delta E \rangle = 2$ kcal mol^{-1}; - - -, $\eta = 0.01$, $\langle \Delta E \rangle = 2$ kcal mol^{-1}. (b) ○, 236.5 nm data;——, $\eta = 0.1$, $\langle \Delta E \rangle = 2$ kcal mol^{-1}; - - -, $\eta = 0.01$, $\langle \Delta E \rangle = 2$ kcal mol^{-1}. The mean energy of *n*-propyl radicals, obtained using the impulsive model, is shown for each calculation.

Fig. 6. Stern–Volmer plots. (a) ○, 236.5 nm data; ——, $\eta = 0.1$, strong collisions; - - -, $\eta = 0.01$, strong collisions. (b) ○, 214 nm data;——, $\eta = 0.1$, strong collisions; - - -, $\eta = 0.01$, strong collisions. The mean energy of *n*-propyl radicals, obtained using the impulsive model, is shown for each calculation.

proximately 2 kcal mol^{-1} wide) separated by 12 kcal mol^{-1}. Figure 5 illustrates calculations with $\eta = 0.01$ and $\eta = 0.10$ for $\Delta E = 2$ kcal mol^{-1} and Fig. 6 illustrates calculations for strong collisions. All calculations exhibit convex curvature and average energies associated with them are feasible.

5. Summarizing remarks

The experiments indicate that propyl radicals with internal excitation are produced during 1-iodopropane photolysis with all four wavelengths, as shown by their unimolecular decomposition. The rates of decomposition increased monotonically with decreasing wavelength, indicating that the amount of excitation the radicals received follows a similar trend. Fitting of the rate data with models based on the lifetime of excited 1-iodopropane gave evidence of a population inversion in iodine atom production during photolysis at all four wavelengths and showed that a statistical model of energy partitioning was inconsistent with the data. An impulsive model can be used to explain the results.

Furthermore, the calculations indicate that the population inversion may be smaller at 214 nm that at longer wavelengths which are in the A band.

Acknowledgment

This work was supported by the U.S. Department of Energy under Contract DE-AC02-76ER02026.

References

1 J. R. Majer and J. P. Simons, *Adv. Photochem.*, *2* (1964) 137.
2 R. E. Rebbert and P. Ausloos, *J. Chem. Phys.*, *47* (1967) 2849.
3 B. G. Dzantiev, I. A. Degterev and A. P. Shvedchikov, *Khim. Vys. Energ.*, *4* (1970) 188.
4 R. E. Rebbert, S. G. Lias and P. Ausloos, *Int. J. Chem. Kinet.*, *5* (1973) 893.
5 S. J. Riley and K. R. Wilson, *Discuss. Faraday Soc.*, *53* (1972) 132.
6 J. V. V. Kasper and G. C. Pimentel, *Appl. Phys. Lett.*, *9* (1964) 231.
7 R. J. Donovan and D. Husain, *Nature (London)*, *209* (1966) 609.
8 T. Donahue and J. R. Wiesenfeld, *J. Chem. Phys.*, *63* (1975) 3130.
9 R. A. Boschi and D. R. Salahub, *Mol. Phys.*, *24* (1972) 289.
10 J. G. Calvert and J. N. Pitts, Jr., *Photochemistry*, Wiley, New York, 1966, p. 798.
11 B. T. Connelly and G. B. Porter, *Can. J. Chem.*, *36* (1958) 1640.
12 A. D. Jenkins, *J. Chem. Soc.*, (1952) 2563.
13 D. Porret and C. F. Goodeve, *Proc. R. Soc. London, Ser. A*, *165* (1938) 31.
14 M. M. Papic and K. J. Laidler, *Can. J. Chem.*, *49* (1971) 549.
15 B. A. Thrush, *Proc. R. Soc. London, Ser. A*, *243* (1958) 555.
16 R. Schindler and M. H. J. Wijnen, *Z. Phys. Chem., Frankfurt am Main*, *34* (1962) 109.
17 C. E. McCauley and G. J. Hilsdorf, *J. Am. Chem. Soc.*, *80* (1958) 5101.
18 J. A. Guercione and M. H. J. Wijnen, *J. Chem. Phys.*, *38* (1963) 1.
19 R. J. Donovan, F. G. M. Hathorn and D. Husain, *Trans. Faraday Soc.*, *64* (1968) 3192.
20 P. J. Robinson and K. A. Holbrook, *Unimolecular Reactions*, Wiley, New York, 1972.
21 W. E. Falconer, B. S. Rabinovitch and R. J. Cvetanovic, *J. Chem. Phys.*, *39* (1967) 40.
22 R. J. Campbell and E. W. Schlag, *J. Am. Chem. Soc.*, *89* (1967) 5103.
23 R. D. Souffie, R. R. Williams, Jr., and W. H. Hamill, *J. Am. Chem. Soc.*, *78* (1956) 917.

Appendix A

Frequencies and a geometry analogous to propane were used for the propyl radical. The following activated molecule frequencies (cm^{-1}) were taken from ref. A1: 372, 748, 870, 930 (2), 1053, 1167 (2), 1278, 1336, 1380, 1462 (4) and 2944.

The radical was assumed to have two free internal rotations with moments of inertia of 4.53×10^{-40} and 2.52×10^{-40} cm^2 with symmetry numbers of 3 and 2 respectively. Activated complex frequencies (cm^{-1}) for C—C rupture were 185 (2), 320, 690 (2), 780, 990 (2), 1255, 1408 (6) and 2985. Activated complex frequencies (cm^{-1}) for C—H rupture were 150, 200, 550, 800, 866 (3), 1044 (3), 1445 (6) and 2995 (6).

Each molecular model has one free internal rotation with moments of inertia of 5.46×10^{-40} and 4.53×10^{-40} g cm^2 and each has a symmetry number of 3. $p_1^*/p_1 = 1.62$ and 1.00 respectively; C—C rupture has one reaction path whereas the C—H split has two possible paths.

TABLE A1

Hard sphere collision diameters

Species	σ (Å)
1-Iodopropane	5.2 (estimated)
Nitrogen	3.7
Propyl radical	5.1 (estimated)

TABLE A2

Thermochemistry

Species	$\Delta H^{\circ}_{f\,298}$ (kcal mol^{-1})
CH_3	34.0
n-C_3H_7	20.7
$CH_2{=}CH{-}CH_3$	4.88
HI	6.27
n-C_3H_7I	−7.1
I	25.54

Threshold energies of 29.7 and 35.4 kcal mol^{-1} were calculated together with values of 4.06 and 3.61 cal K^{-1} mol^{-1} for the entropy of activation. The values 29.7 kcal mol^{-1} and 4.06 cal K^{-1} mol^{-1} were in agreement with data given in ref. A2, and the values 35.4 kcal mol^{-1} and 3.61 cal K^{-1} mol^{-1} were in agreement with data given in ref. A3.

Additional data are given in Tables A1 and A2.

References for Appendix A

A1 W. E. Falconer, B. S. Rabinovitch and R. J. Cvetanovic, *J. Chem. Phys.*, *39* (1967) 40.
A2 M. M. Papic and K. J. Laidler, *Can. J. Chem.*, *49* (1971) 535.
A3 W. M. Jackson and J. R. McNesby, *J. Am. Chem. Soc.*, *83* (1961) 4891.